



# Comparison of EUV Photomask Metrology Between CD-AFM and TEM

Gaoliang Dai<sup>1</sup> · Kai Hahm<sup>1</sup> · Lipfert Sebastian<sup>2</sup> · Markus Heidelmann<sup>3</sup>

Received: 3 November 2021 / Revised: 5 January 2022 / Accepted: 7 January 2022 / Published online: 3 February 2022  
© The Author(s) 2022, corrected publication 2022

## Abstract

Accurate metrology of extreme ultraviolet (EUV) photomask is a crucial task. In this paper, two different methods for reference EUV photomask metrology are compared. One is the critical dimension atomic force microscopy (CD-AFM). In the measurements, the contribution of its AFM tip geometry is usually the dominant error source, as measured AFM images are the dilated results of measured structures by the AFM tip geometry. To solve this problem, a bottom-up approach has been applied in calibrating the (effective) AFM tip geometry where the result is traceably calibrated to the lattice constant of silicon crystals. The other is transmission electron microscopy (TEM). For achieving measurement traceability, structure features are measured in pairs in TEM images; thus the distance between the structure pair calibrated by a metrological AFM in prior can be applied to determine the magnification of the TEM image. In this study, selected photomask structures are calibrated by the CD-AFM, and then sample prepared and measured by high-resolution TEM nearly at the same location. The results are then compared. Of six feature groups compared, the results agree well within the measurement uncertainty, indicating excellent performance of the developed methodology. This research supports the development of a photomask standard, which is applied as a “reference ruler” with improved low measurement uncertainty in photomask fabs.

**Keywords** Extreme ultraviolet (EUV) photomask standard · Traceable calibration · Metrology · Critical dimension (CD) · Atomic force microscopy (AFM) · Transmission electron microscopy (TEM) · High precision · Low measurement uncertainty

## 1 Introduction

Extreme ultraviolet lithography (EUVL) is a lithography technology which uses extreme ultraviolet (EUV) radiation with a wavelength of 13.5 nm. Current EUVL systems, equipped with optical systems with a numerical aperture (NA) of 0.33, are entering high-volume manufacturing. Intensive developments are being carried out in realizing EUV tools with a higher NA of 0.55 [1], thus for extending Moore’s law throughout the next decade. In EUV lithography, the designed feature patterns are firstly manufactured on EUV photomasks, which are then transferred to wafers

with a designed zoom factor (currently 4:1 for EUVL with NA = 0.33). The development of EUV photomasks has challenges. For instance, due to the short wavelength of the EUV radiation, the absorption (and thus the energy loss of the EUV light) is one of the biggest challenges in EUVL. To mitigate this problem, photomasks with alternative materials to the commonly used Mo/Si multilayer (ML) reflector and patterned Ta-based absorber (both of which are known to require shadow effect corrections and lead to large through-focus pattern placement errors) are being actively explored [2].

To satisfy the process needs of ever-smaller technology nodes, the tolerance of dimensional parameters of manufactured feature patterns of EUV photomasks is also becoming tighter. Such dimensional parameters to be controlled include line width (often synonymously named as critical dimension, CD), CD uniformity (CDU), pitch, height, sidewall angle, line edge/width roughness (LER/LWR). Furthermore, as high-resolution electron beam lithography (EBL) is usually applied in photomask manufacturing, it often suffers from, e.g., proximity effect [3] and fogging effect. For

✉ Gaoliang Dai  
gaoliang.dai@ptb.de

<sup>1</sup> Physikalisch-Technische Bundesanstalt,  
38116 Braunschweig, Germany

<sup>2</sup> Advanced Mask Technology Center GmbH & Co. KG,  
01109 Dresden, Germany

<sup>3</sup> ICAN, Universität Duisburg-Essen, 47057 Duisburg,  
Germany

quality-management purposes, usually a kind of photomask standard is applied in photomask fabs, which serves as a “reference” for traceability of CD measurements. Before its application, however, the dimensional parameters of reference patterns of the photomask standards need to be calibrated accurately and traceably.

Various measurement technologies such as atomic force microscopy (AFM), scanning electron microscopy (SEM), and optical and X-ray scatterometry are available today for measuring dimensional parameters of nanostructures [4]. However, there are still significant challenges for applying these for accurate and traceable metrology. The AFM technique applies a very small AFM tip with a radius down to a few nanometers in scanning nanostructures. It has advantages of, for example, high vertical and lateral resolution, being (almost) non-destructive, (quasi-)3D, and capable of being measured in liquid, ambient, and vacuum. However, AFM images are the dilated results of nanostructures by the applied AFM tip geometry [5]. To determine the true structure geometry from measured AFM images, the contribution of the AFM tip geometry needs to be corrected, typically by using the morphological operation of erosion. Thus, the accurate and traceable characterization of the tip geometry [6] and control of tip wear [7] in measurements becomes a critical issue. In addition, AFM is typically slow, and it is hard to measure highly dense patterns due to the limit of the tip. SEM scans a finely focused electron beam over the sample, where the secondary electrons (SE), backscattered electrons (BSE), and/or other signals can be acquired to image feature shape, size, and/or composition with a resolution down to sub-nanometer scale. Owing to fast measurement speed and high resolution, the SEM technique is one of the most versatile techniques used in semiconductor manufacturing today. However, to achieve accurate and optimum results, prior knowledge of the 3D geometry of the structures is also necessary for SEM to interpret the SE edge bloom [8]. Optical and X-ray scatterometry measures the dimensions of periodical nanostructures by analyzing their diffraction patterns [9]. Its measurement is fast and non-invasive, and thus applicable for in situ measurement applications.

However, scatterometry has challenges in resolving the dimensional parameters from the measured diffraction pattern, an issue known as the inverse problem. Such challenges include, for instance, the requirement of prior knowledge of the 3D geometry of the structures and the so-called multiple minima (ambiguities) issue [10]. A significant challenge remains today that there is often measurement inconsistency between different metrology techniques/tools.

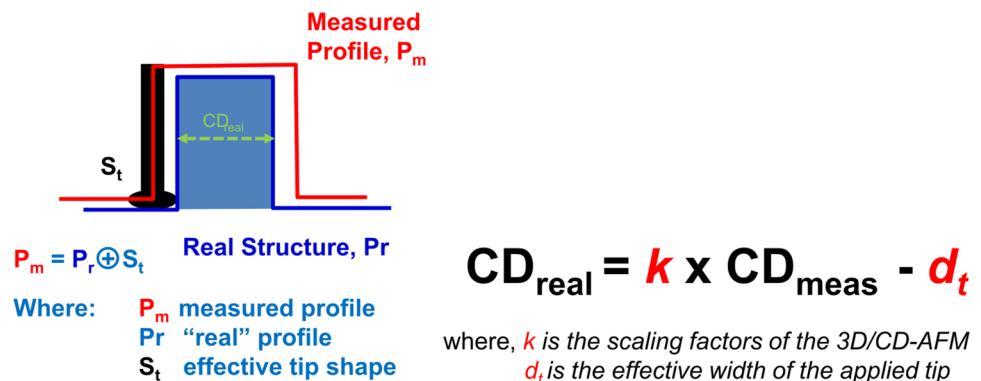
Recently, a EUV photomask standard has been developed. For sake of protecting industrial know-how, this paper focuses on the introduction of the methodology developed for accurate and traceable metrology of the EUV photomask. In this paper, Sects. 2 and 3 detail the traceable calibration of the developed standard using the CD-AFM technique with a bottom-up traceability approach – an approach using the lattice constant of crystal silicon as a natural ruler for traceable nanometrology. Section 4 introduces a comparison between the AFM and transmission electron microscopy (TEM) measurements of a selected photomask to verify the calibration results.

## 2 Concept of Bottom-Up Traceability Approach

Traceability is a fundamental issue for nano-dimensional metrology. The lack of traceability in measurements inhibits the comparison of tools from different manufacturers (known as the tool-to-tool matching issue) and limits knowledge about the real size of fabricated features [11].

Generally speaking, there are two categories of issues in realizing accurate and traceable calibration of nanostructures using microscopic techniques: (i) the calibration of the length scales, and (ii) the determination of edge position of structures from measured image. For AFM measurements, these two issues are represented as the calibration of the scaling factors,  $k$ , of the AFM scanner and of the (effective) tip geometry,  $d_t$ , as shown in Fig. 1. For electron microscopic measurements, the issues can be understood as the calibration of the magnification factor of the SEM (or TEM)

**Fig. 1** Schematic diagram showing two fundamental metrology tasks for traceable nanodimensional metrology: (1) calibration of the scaling factors and (2) calibration of the effective tip/probe width



and the interpretation of the SEM image in determining the feature edges.

Thanks to the development of state-of-the-art metrological AFMs [12, 13], currently the calibration of the scaling factors of AFMs (or the magnification of SEM/TEM [14]) can be performed with a relative uncertainty of better than  $10^{-3}$ . Consequently, its contribution to the overall measurement uncertainty of CD metrology is typically insignificant, especially for small features of the current technology node [15]. Following the miniaturization of nanostructures in manufacturing, however, the influence of tip geometry becomes increasingly important, and very often becomes the most dominant factor in the uncertainty budget of CD metrology. Therefore, the accurate and traceable calibration of tip geometry remains a big challenge today for nanometrology.

A bottom-up traceability approach has recently been developed by several national metrology institutes [16–18] for nanometrology. The key concept of the approach is to apply the crystal lattice constant as an internal ruler for traceable nanometrology. In the simplified schematic diagram shown in Fig. 2a, for example, the feature width would be calculated as the number ( $N$ ) of crystal lattice planes within the feature’s cross section multiplied by the silicon crystal constant  $a_{111}$ . This constant  $a_{111}$  has been traceably measured as 313.560 11(17) pm for silicon through a combination of X-ray and optical interferometry [19]. This approach was recently recommended as a secondary realization of the meter for nanometrology by the Consultative Committee for Length (CCL) of the Bureau International des Poids et Mesures (BIPM) [20]. State-of-the-art high-resolution transmission electron microscopy

(HR-TEM) is capable of resolving the spatial periodicity of a crystal lattice, as illustrated in a measurement example in Fig. 3.

The realization of the bottom-up traceability approach has been systematically studied and published elsewhere [16–18, 21, 22]. For sake of completeness of this paper, two important issues are introduced in the following context.

The first issue concerns the dissemination of the TEM measurement results of silicon samples to calibration applications. This issue is related to the fact that the sample needs to be destructively prepared into thin “lamella” so that it can be measured by TEM. Consequently, the feature is no longer available for further calibration applications. To solve this problem, a strategy based on the data fusion concept is applied as explained in Fig. 2b [21]. The strategy applies two groups of specimens, one as the reference structures and the other as the TEM target structures. Whole measurement procedures consist of three steps. First, the difference of the CD of the two specimens is measured by, e.g., a CD-AFM. Second, the TEM target is destructive sample prepared and measured by a TEM to determine its true dimensions using the bottom-up approach mentioned above. Third, the data of the two steps are fused to determine the geometry of the reference structure. The benefit of this approach is that the reference structure is available for reference metrology as no destructive sample preparation is needed for it. The challenge issue is that the overall measurement uncertainty is a combination of measurement uncertainties of all steps, as illustrated in Fig. 2b. Consequently, each step needs to be performed as accurate as possible to achieve the best possible metrology.

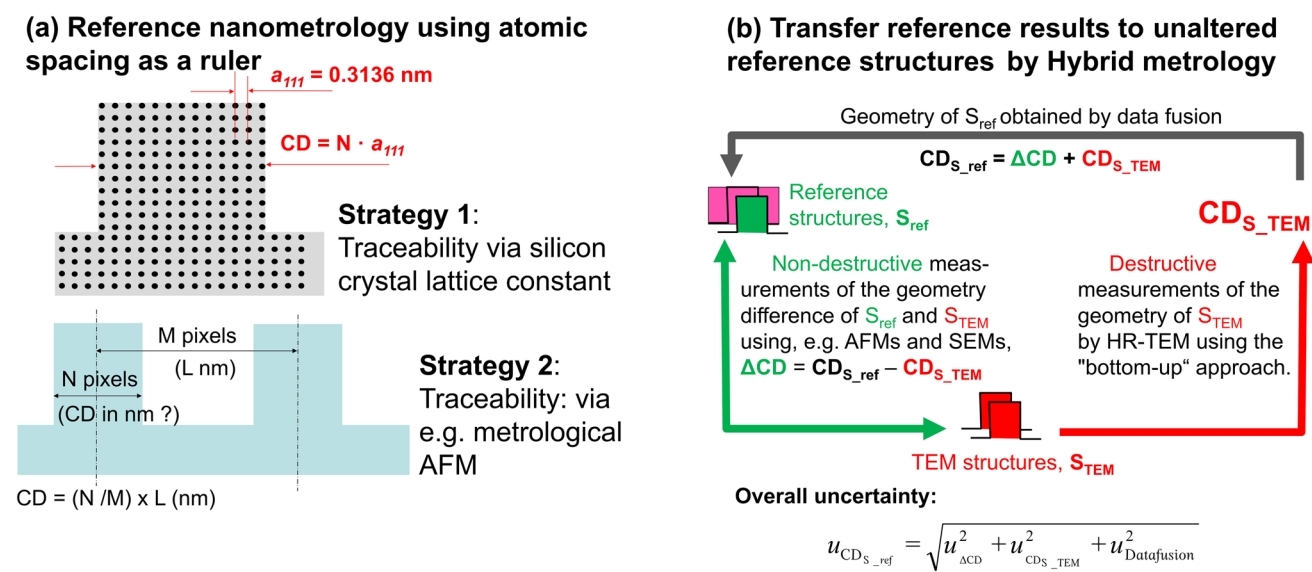
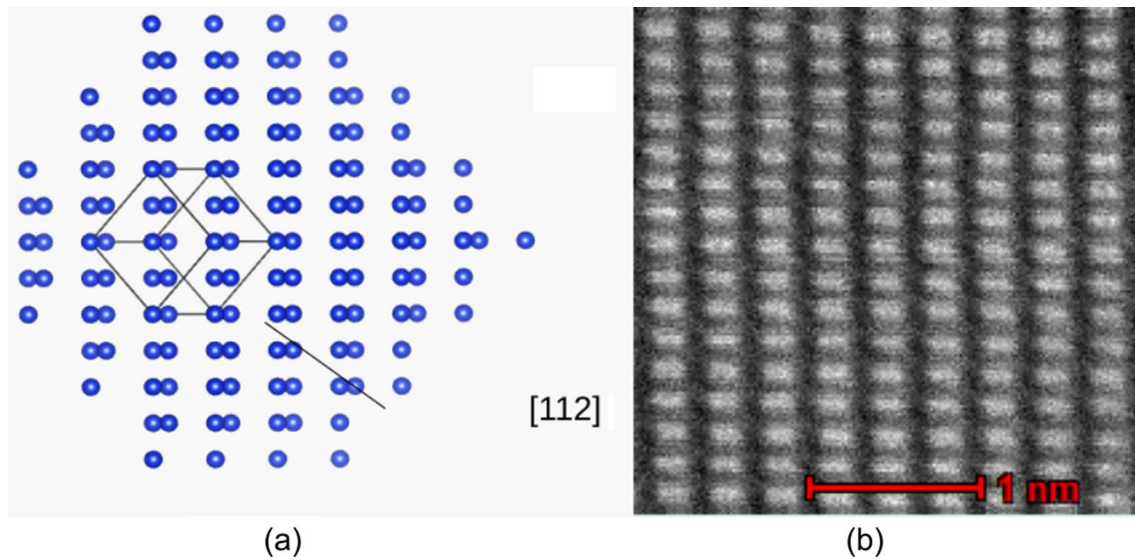


Fig. 2 Concept of the bottom-up approach for traceable nanodimensional metrology [21]



**Fig. 3** **a** Crystalline structure of silicon [112] and **b** measured TEM of crystalline structure of silicon [112] by a TEM type “Titan Themis 300” under an image magnification of 10Mx, and a resolution of 8 pm/pixel

The other issue concerns the constraints of materials in applying the bottom-up approach. As the crystal lattice needs to be applied as a ruler in measurements, basically the bottom-up approach requires the structure to be made of crystal materials. However, this requirement cannot be satisfied for (EUV) photomasks. To overcome this problem, an adapted method based on a calibrated pitch has also been developed [17]. Its concept is illustrated in strategy 2 of Fig. 2a. The pitch  $p$  of line features was accurately and traceably calibrated as  $L$  nm before the sample was destructively prepared, for instance, by use of a metrological AFM [12]. Then, the line features can be sacrificed for sample preparation and TEM measurements. From the TEM images, the pitch and width of the feature pair could be determined in units of pixels (illustrated as  $M$  and  $N$  pixels in the figure, respectively). By combining the TEM and AFM measurement results, the scaling factor of the TEM image can be calculated as  $k = L/M$  (nm/pixel) and the widths of the structures can be evaluated as  $N \times L/M$  (nm). An important idea underlying the proposed method is that unlike the CD metrology, the pitch calibration using AFMs is tip geometry-independent.

The results of state-of-the-art studies indicate that sub-nanometer measurement uncertainty can be reached for CD metrology using reference TEM method [18]. When the error propagation of all possible error sources in both realization and dissemination is considered, the expanded measurement uncertainty of CD metrology may reach about 0.7–1.6 nm using the methodology mentioned above, as confirmed in a bilateral comparison between the NIST and PTB [22].

### 3 Measurement Result of EUV Photomask Standards Using CD-AFM

The developed EUV photomask standards are measured by an advanced CD-AFM developed at PTB. The development of the CD-AFM is introduced in detail elsewhere [23], therefore only a brief introduction is given here. The AFM uses the classic optical lever technique to detect the bending and torsion of the cantilever. The AFM measurements are mostly performed in the intermittent-contact mode, where the amplitude modulation technique is applied for detecting the tip-sample interaction. For achieving better CD measurement performance, a new probing and measurement strategy, referred to as the vector approaching probing (VAP) method, has been developed. The displacement scaling factors of the AFM scanner are traceably calibrated using a set of step height and lateral standards that were measured by the PTB metrological large-range AFM [12] with a relative calibration uncertainty of about 0.1%.

Primarily two types of CD tips were applied: CDR-EBD (Nanotools) tips with the flared tip made of diamond-like carbon (DLC) and CDR (Team nanotech) tips made of silicon. Tips having nominal widths of 30, 70, and 120 nm were used. A calibration cycle was performed with two or three repeated measurement runs. A new tip was installed at the beginning of each measurement run. The (effective) tip geometry is then calibrated by measurement of the PTB master CD standards type IVPS100-PTB [21], whose geometry is traceably calibrated using

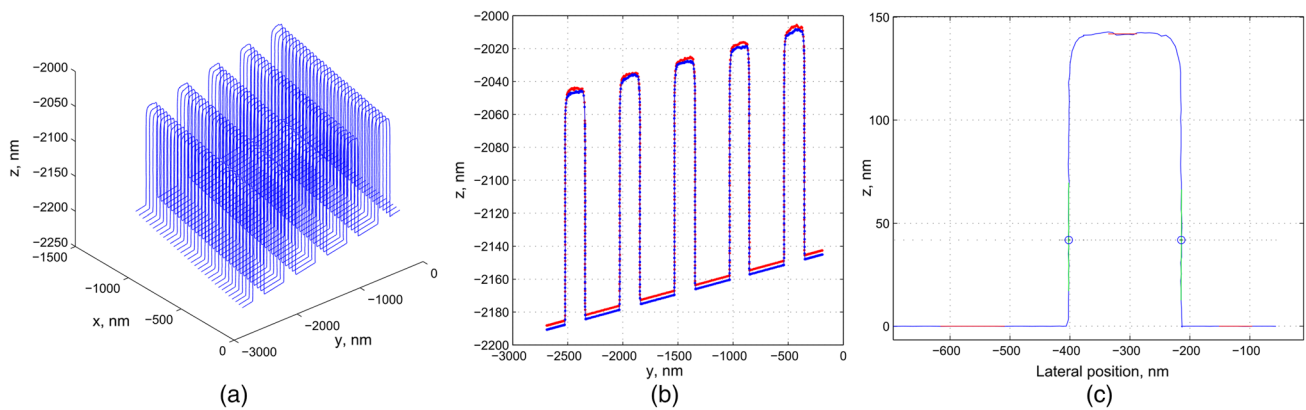


**Fig. 4** Calibration of effective tip width using a PTB reference CD standard, shown as **a** 3D-view of an AFM image of the CD standards shown as raw data; **b** two cross-sectional profiles of the AFM image shown in (a); **c** the evaluation of the apparent feature width of the CD standard

the bottom-up traceability approach as mentioned above. A typical measurement image of such calibration is shown in Fig. 4 as an example. Based on this method, either the effective tip width or tip geometry can be characterized with sub-nanometer repeatability [6]. Its result can then be applied to correct the measurements of the target features of the photomask standard.

It should be stressed that the effective tip geometry calibrated above included both the actual geometry of the tip and the effect of the tip sample interaction, and these two contributions are importantly different [24]. The actual tip geometry is independent of the sample and the measurement conditions, excluding the possible effect of tip wear. In contrast, the tip-sample interaction can depend significantly upon the sample and measurement conditions. Therefore, in this study, all instrument scan and control parameters were held constant during the whole measurement runs to minimize the influence of tip-sample interaction. To monitor the tip wear, the master CD standards were also measured during and after the target measurements. The observed tip wear was very small. Typically, the change in effective tip width during each measurement cycle was less than 0.2 nm, indicating high measurement stability and low tip wear.

After the (effective) tip geometry has been calibrated using the master CD standards, it can be applied to measure nanostructures of EUV photomask standards. As an example, a CD-AFM image measured on a dense dark (DD) pattern with a nominal line width in the range of 100 nm is shown as raw data without tip correction in Fig. 5a. The measurement was performed with a CDR 30-EBD tip, whose effective tip width was calibrated to be 36.8 nm. A typical cross-sectional profile, following a first-order leveling of the data, is shown in Fig. 5b. The edge definition is intended to represent the lateral position of the sidewall of structures at the middle height. However, due to the influence of the so-called vertical edge height

(VEH) of the flared AFM tip, the edge positions are evaluated at the position of (middle height – VEH) [15], where the VEH is taken as 10 nm in this example. To suppress the influence of the measurement noise, a linear fit was performed to a portion of the sidewall around the target point. The slope of this fit line can be taken as the measurement result of the sidewall slope. Edge positions are then calculated from the intersections, marked as EL and ER in Fig. 5(b). The distance between EL and ER gives the apparent CD of the feature. In addition, the variation of the edge positions along successive profiles tells the information about LER/LWR.

To correct the tip contribution, in this paper we applied a simplified method where the CD value of the photomask line feature is determined by subtracting the characterized (effective) tip width from the evaluated (apparent) CD value. The reason is that the line feature has an almost vertical sidewall and thus its higher order tip effect [11] is almost neglectable. It offers advantage of simplicity and fast calculation. Alternatively, the contribution of the characterized tip geometry can be corrected using the morphological operator “erosion” as detailed in our previous study [6].

Several calibrations have been performed on the photomask standard using the method described above. In Fig. 6, the calibration results of a group of isolated dark (ID) lines with nominal width in the range of < 100 nm to 1000 nm are plotted. The expanded measurement uncertainty is about  $\pm 2.5$  nm (95% confidential level). In addition, Table 1 shows the calibrated CD values of two grating patterns each measured at nine locations, indicating a very good CD uniformity, and thereby providing an excellent approach for calibration of several tools over a long time as it mitigates the issue of degradation by repeated measurements.

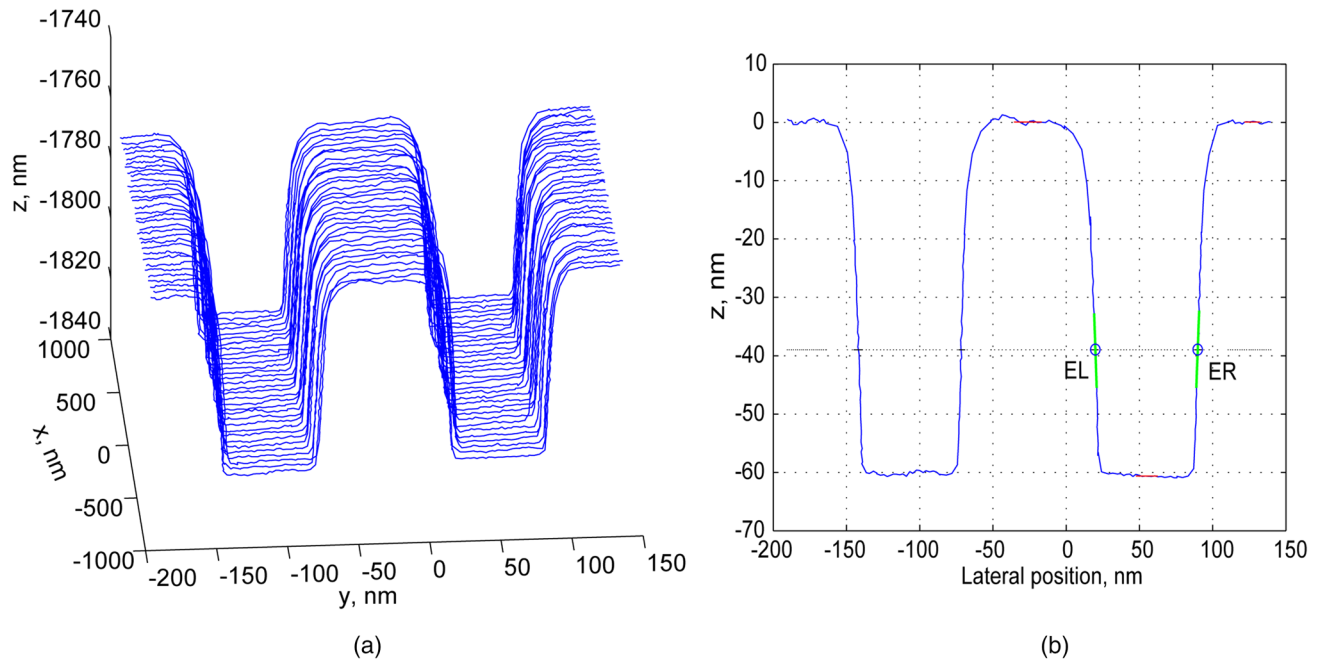


**Fig. 5** AFM image measured on the DD pattern with nominal CD in the range of 100 nm of a photomask standard, shown as the raw data without tip correction in (a); and the evaluation of a cross-sectional profile for middle CD and sidewall angle as shown in (b)

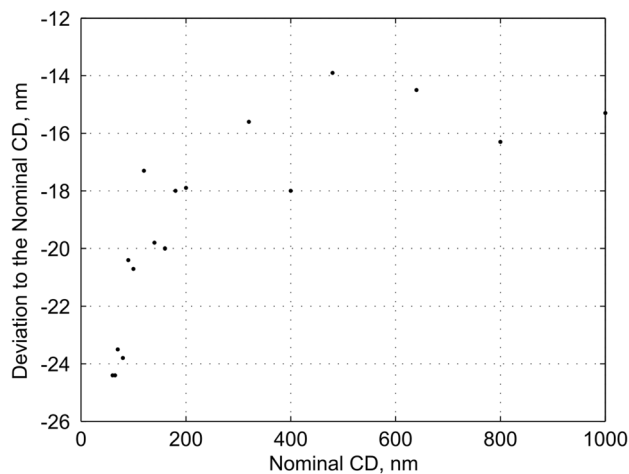


**Fig. 6** Deviation of the calibrated middle CD to its nominal value of a group of isolated dark line patterns with nominal width in the range of < 100 nm to 1000 nm

#### 4 Verification: Comparison of EUV Photomask Metrology Between CD-AFM and TEM

To verify the measurement results obtained by the methodology mentioned above, a comparison on EUV photomask metrology has been performed between the CD-AFM and TEM techniques. Two EUV photomasks are applied in

**Table 1** Calibrated middle CD values of nine measurement positions on two grating patterns, indicating a good CDU

Measurement positions	P160L75	P160L85
A1	63.0	73.4
A2	62.8	73.0
A3	62.5	73.4
B1	62.8	73.2
B2	62.8	73.3
B3	62.7	73.0
C1	62.4	73.8
C2	62.4	73.5
C3	62.5	73.9

All data are given intentionally in arbitrary unit for sake of protecting industrial know-how

the study: one as the reference photomask and the other as the TEM photomask. The procedures of the whole study are illustrated in Fig. 7. The experiment starts from the measurement of two photomasks using CD-AFM, the same as the measurement procedures mentioned in Sect. 4 and marked as steps “S1”, “S2”, “S3” and “S4” in Fig. 7. After performing these measurements, CD-AFM results of two photomasks can be obtained, registered as D1 and D2 in the used database, respectively.

After CD-AFM measurements were finished, the TEM photomask was mechanically cut into segments (“S5”). The photomask segments are then prepared using a commercial

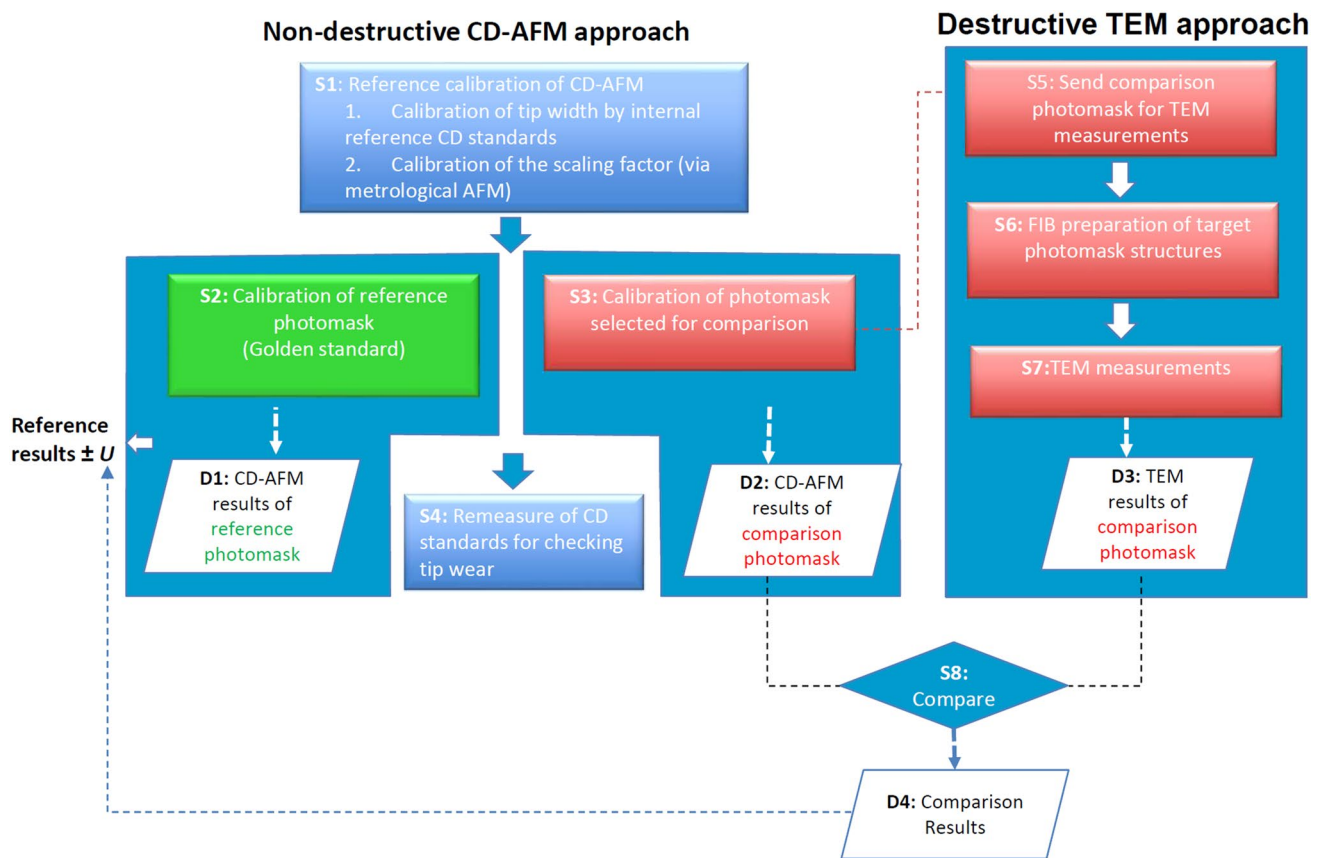


**Fig. 7** Schematic diagram showing the concept of the comparison study of EUV photomask metrology between CD-AFM and TEM

dual beam focused ion beam (FIB) tool to make the TEM “lamella” needed for TEM measurements (“S6”). Great attention is paid in the sample preparation so that the lamella prepared nearly at the same location as the CD-AFM measurements were taken. The TEM measurements (“S7”) are performed using the measurement strategy 2 (Fig. 2a) as detailed in Sect. 3. The obtained TEM measurement results of the TEM photomask (“D3”) are then compared to that of the CD-AFM (“D2”). The result of the comparison (“D4”) is applied to verify the final measurement uncertainty of the calibrated result of the reference photomask. It is to be mentioned that the photomask is cut into smaller sample pieces prior to FIB lamella preparation. This is due to sample size limitations of the applied FIB tool.

A large number of measurements on the prepared photomask lamellas were performed using the scanning transmission electron microscopy (STEM) mode. Images acquired by the high-angle annular dark-field (HAADF) detector are recorded. As an example, two STEM images taken on a line pattern No. R1C12B4H120T1P4 are illustrated in Fig. 8, measured with a magnification of (a) 1Mx and (b) 300kx, respectively. From these STEM images, multilayer features of the EUV photomask for enhancing

the EUV reflectivity are clearly visible. In addition, it can be clearly seen that the photomask structure has almost vertical sidewalls, and has a certain corner rounding and footing at its top and bottom region.

The evaluation of the measured STEM image for traceable CD metrology is illustrated in Fig. 8b, following the concept detailed already in Sect. 2. In order to have a good comparison with the results of CD-AFM measurements, the CD at the middle height of the feature is evaluated. In the evaluation, first the height of the feature is calculated. Then, the positions of left and right edges ( $X_{L1}$ ,  $X_{R1}$ ,  $X_{L2}$  and  $X_{R2}$ ) of two structures ( $X_{c1}$  and  $X_{c2}$ ) can thus be calculated as  $(X_{L1} + X_{R1})/2$  and  $(X_{L2} + X_{R2})/2$ , respectively; and the distance (i.e., pitch) of the two structures be calculated as  $L = X_{c2} - X_{c1}$ . Note that, so far, all evaluation results are in units of pixel only, i.e., not in a real length scale. By combining the pitch values measured by the TEM (i.e.,  $L$  pixels) and the CD-AFM (e.g.,  $P$  nm), the magnification of the TEM can be determined as  $k = P/L$  nm/pixel and the above evaluated results (in pixels) can be converted into real length scale by multiplying the evaluated scaling factor  $k$ .

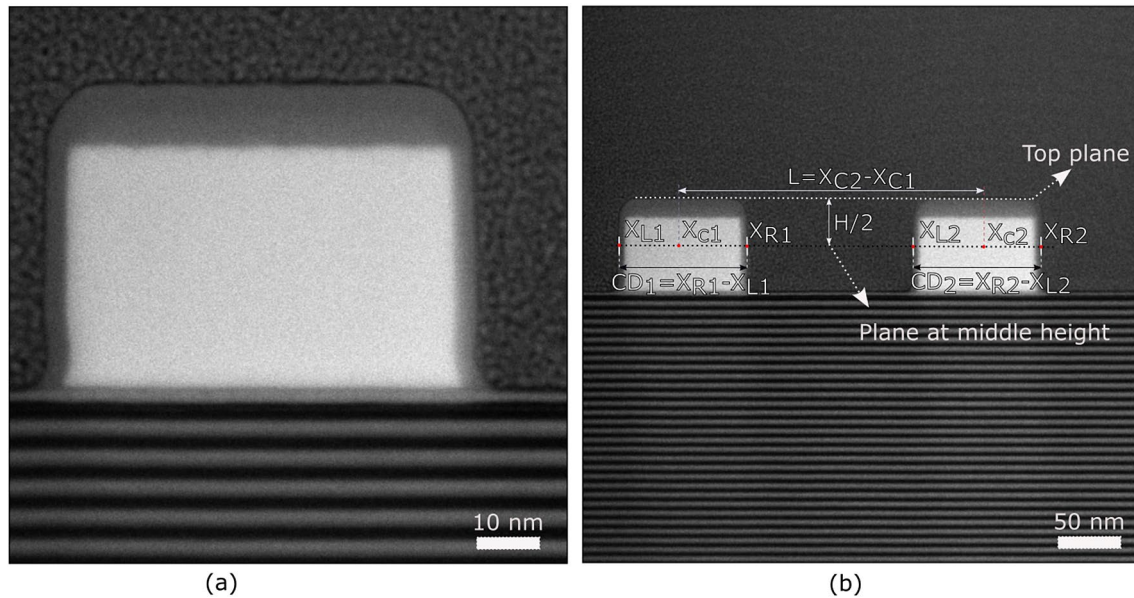


**Fig. 8** TEM image of an EUV photomask line pattern (No. R1C12B4H120T1P4) measured with a magnification of 1Mx (a) and a magnification of 300kx (b)

**Table 2** Comparison of middle CD values measured by the CD-AFM and TEM. All data are in nm

	CD-AFM	$U_{CD\_AFM}$	TEM	$\sigma_{TEM}$	AFM-TEM
R1C12T1H120	104.7	2.5	105.8	2.1	-1.1
R1C12T1H140	124.7	2.5	123.2	2.3	1.5
R1C12T1H160	145.2	2.5	142.8	2.3	2.4
R1C12T1H180	163.2	2.5	162	2.0	1.2
R1C12T1H200	183.9	2.5	184.0	2.6	-0.1
R1C12T1H320	302.1	2.5	303.1	1.7	-1.0

The comparison results of CD-AFM and TEM are summarized in Table 2 and depicted in Fig. 9. The expanded measurement uncertainty of the CD-AFM is estimated as 2.5 nm (95% confidential level). To illustrate the quality of the TEM measurements, the standard deviation of its measurement results is applied (the reason for this will be detailed later). It can be seen that the agreement of two (principally different) methods is excellent: for six feature groups compared the deviation is well below the estimated measurement uncertainty, confirming the feasibility of the developed methodology.

To have a deeper understanding of the possible reasons for the observed deviation, an important issue concerning the principal differences of two measurements (e.g., measurement range and resolution) needs to be discussed. Although great attention was given in preparing TEM lamella at nearly the same location as the CD-AFM measurement took place, inevitably there are deviations in reality due to subtle

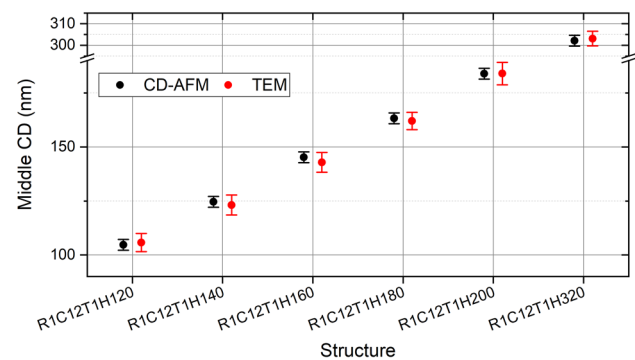


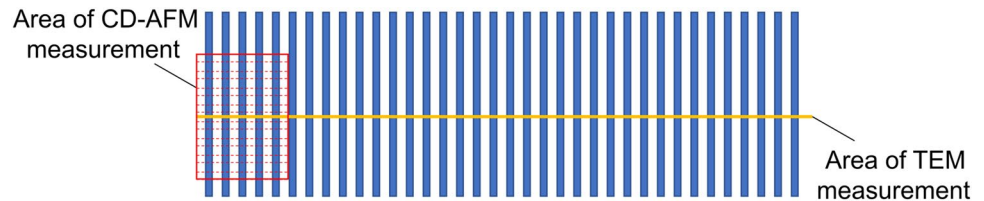
**Fig. 9** Comparison of middle CD values measured by the CD-AFM and STEM. The error bar of the CD-AFM indicates the extended measurement uncertainty ( $k=2$ ). The error bar of the TEM indicates two times of the standard deviation of the CD values of multiple features evaluated by STEM

positional differences. In addition, the measurement areas of two methods are significantly different, as illustrated in Fig. 10. In AFM measurements, we are measuring in a rectangular area with a size of approximately  $1.2 \mu\text{m} \times 1.0 \mu\text{m}$ , proving AFM images with  $620 \text{ pixels/line} \times 16 \text{ lines}$ . From one image, 80 (i.e.,  $5/\text{line} \times 16 \text{ lines}$ ) CD values in total can be evaluated. In contrast, the TEM lamella prepared is very thin (below 100 nm). From the STEM image, we can only obtain one CD value per line feature. Consequently, the difference in measurement location, area, and resolution of two methods may result in measurement deviation.

To mitigate the problem mentioned above, in the comparison we are comparing the averaged values of the



**Fig. 10** Schematic drawing showing that the results of CD-AFM and TEM measurements represent different areas of the feature pattern, which may lead to measurement deviation



CD-AFM and TEM measurements. The CD-AFM result is taken as the mean value of 80 evaluated CD values, as mentioned above. The standard deviation of 80 CD values is about  $\sigma_{\text{AFM}} = 2.7$  nm. Its contribution, which is evaluated as  $(\sigma_{\text{AFM}}/\sqrt{n})$ , where  $n=80$ , has been included in the measurement uncertainty  $U_{\text{CD\_AFM}}$  given in Table 2. In the TEM measurement, we have taken TEM images over multiple structure pairs (i.e., structure pairs of line No. 1 + 2, 2 + 3, 3 + 4, ... 31 + 32). From the STEM image of each structure pair, we can evaluate CD values of two structures. Thus, in total, we obtain 32 CD values of 32 structures from the STEM images. Finally, the averaged value of 32 STEM results is applied for comparison. The standard deviation of 32 STEM results is detailed as  $\sigma_{\text{TEM}}$  in Table 2. The benefit of this approach is that the statistically averaged value is advantageous to depress the influence of local variation of the measured CD values which is (partly) attributed to e.g., LER/LWR of structures. As an indicator of the measurement quality of TEM results, we have applied the standard deviation of 32 STEM results in Table 2 and Fig. 9.

## 5 Conclusions

EUV lithography is the enabling technology for extending Moore's law throughout the next decade. The miniaturization of nanostructures demands ever-tighter tolerance in the manufacturing of EUV photomasks. For ensuring manufacturing quality, CD standards play an important role in manufacturing, e.g., to trace, calibrate, and verify measurement systems. This paper introduces the development and traceable calibration of EUV photomask standards.

CD-AFM has been applied for the accurate and traceable calibration of the EUV photomask standard. For ensuring measurement traceability, the scaling factor of the tool is calibrated to a metrological AFM which has displacement interferometry incorporated into the scanners. Thus, its results are traceable to the SI meter via the calibration of its laser wavelength. To correct the contribution of (effective) tip geometry of AFM, a bottom-up approach is applied where the result is traceable to the SI unit meter via the lattice constant of silicon crystal. Detailed measurement results of the EUV photomask standard have been presented in the paper.

To verify the measurement results, a comparison between CD-AFM and TEM has been performed. Its results agree well within the measurement uncertainty, indicating the feasibility of the developed methodology. The residual deviation of the comparison results is (partly) attributed to the different measurement conditions (i.e., location, range, and resolution) of two methods.

**Funding** Open Access funding enabled and organized by Projekt DEAL.

**Conflict of interest** Gaoliang Dai is an editorial board member for "Nanomanufacturing and Metrology" and was not involved in the editorial review, or the decision to publish, this article. All authors declare that there are no competing interests.

**Open Access** This article is licensed under a Creative Commons Attribution 4.0 International License, which permits use, sharing, adaptation, distribution and reproduction in any medium or format, as long as you give appropriate credit to the original author(s) and the source, provide a link to the Creative Commons licence, and indicate if changes were made. The images or other third party material in this article are included in the article's Creative Commons licence, unless indicated otherwise in a credit line to the material. If material is not included in the article's Creative Commons licence and your intended use is not permitted by statutory regulation or exceeds the permitted use, you will need to obtain permission directly from the copyright holder. To view a copy of this licence, visit <http://creativecommons.org/licenses/by/4.0/>.

## References

1. Van Schoot J, van Setten E, Troost K et al (2020) High-NA EUV lithography exposure tool: program progress. In: Proceedings of SPIE. Extreme ultraviolet (EUV) lithography XI, vol 11323, p 1132307, <https://doi.org/10.1117/12.2551491>
2. Wood O, Wong K, Parks V et al (2016) Improved Ru/Si multilayer reflective coatings for advanced extreme ultraviolet lithography photomasks. BACUS—The International Technical Group of SPIE Dedicated to the Advancement of Photomask Technology 32(6)
3. Maurer W, Friedrich CM, Mader L, Thiele J (1999) Proximity effects of alternating phase-shift masks. In: Proceedings of SPIE. 19th annual symposium on photomask technology, vol 3873. <https://doi.org/10.1117/12.373330>
4. Orji NG, Badaroglu M, Barnes BM et al (2018) Metrology for the next generation of semiconductor devices. Nat Electron 1:532–547. <https://doi.org/10.1038/s41928-018-0150-9>
5. Dahlen G, Osborn M, Okulan N, Foreman W, Chand A (2005) Tip characterization and surface reconstruction of complex structures with critical dimension atomic force microscopy. J Vac Sci Technol B 23:2297–2303

6. Dai G et al (2020) Accurate tip characterization in critical dimension atomic force microscopy. *Meas Sci Technol* 31:074011
7. Strahlendorff T, Dai G, Bergmann D et al (2019) Tip wear and tip breakage in high-speed atomic force microscopes. *Ultramicroscopy* 201:28–37
8. Frase CG, Buhr E, Dirscherl K (2007) CD characterization of nanostructures in SEM metrology. *Meas Sci Technol* 18:510
9. Raymond CJ et al (1995) Metrology of subwavelength photorealist gratings using optical scatterometry. *J Vac Sci Technol B* 13:1484–1495
10. Bodermann B, Wurm M, Diener A, Scholze F, Gross H (2009) EUV and DUV scatterometry for CD and edge profile metrology on EUV masks. In: EMLC'09 25th European mask and lithography conference, pp 1–12
11. Orji NG, Dixson RG (2007) Higher order tip effects in traceable CD-AFM based linewidth measurements. *Meas Sci Technol* 18:448–455
12. Dai G, Wolff H, Pohlenz F, Danzebrink HU (2009) A metrological large range atomic force microscope with improved performance. *Rev Sci Instrum* 80:043702
13. Misumi I, Dai G, Lu M et al (2010) Bilateral comparison of 25 nm pitch nanometric lateral scales for metrological scanning probe microscopes. *Meas Sci Technol* 21:035105
14. Deng X, Dai G, Liu J et al (2021) A new type of nanoscale reference grating manufactured by combined laser-focused atomic deposition and x-ray interference lithography and its use for calibrating a scanning electron microscope. *Ultramicroscopy* 226:113293
15. Dai G, Hahm K, Scholze F et al (2014) Measurements of CD and sidewall profile of EUV photomask structures using CD-AFM and tilting-AFM. *Meas Sci Technol* 25:044002
16. Orji NG, Dixson RG, Garcia-Gutierrez DI, Bunday BD, Bishop M, Cresswell MW, Allen RA, Allgair JA (2016) TEM calibration methods for critical dimension standards. *J. Micro/Nanolith MEMS MOEMS* 15:044002
17. Dai G, Heidelmann M, Kübel C, Prang R, Flügge J, Bosse H (2003) Reference nano-dimensional metrology by scanning transmission electron microscopy. *Meas Sci Technol* 24:085001
18. Kobayashi K, Misumi I, Yamamoto K (2021) Experimental evaluation of uncertainty in sub-nanometer metrology using transmission electron microscopy due to magnification variation. *Meas Sci Technol* 32:095011
19. Massa E et al (2009) Measurement of the lattice parameter of a silicon crystal. *New J Phys* 11:053013
20. Yacoot A, Bosse H, Dixson R (2020) The lattice parameter of silicon: a secondary realisation of the metre. *Meas Sci Technol* 31:121001
21. Dai G, Zhu F, Heidelmann M, Fritz G, Bayer T, Kalt S, Flügge J (2015) Development and characterisation of a new linewidth reference material. *Meas Sci Technol* 26:115006
22. Dai G et al (2017) Comparison of line width calibration using critical dimension atomic force microscopes between PTB and NIST. *Meas Sci Technol* 28:065010
23. Dai G, Häbeler-Grohne W, Hüser D, Wolff H, Flügge J, Bosse H (2012) New developments at Physikalisch-Technische Bundesanstalt in three-dimensional atomic force microscopy with tapping and torsion atomic force microscopy mode and vector approach probing strategy. *J Micro/Nanolith MEMS MOEMS* 11:011004
24. Dixson R, Orji N, Misumi I, Dai G (2018) Spatial dimensions in atomic force microscopy: Instruments, effects, and measurements. *Ultramicroscopy* 194:199–214